Coordination Chemistry of Nitrile and Amino Pendant Arm Derivatives of [9]aneN$_2$S and [9]aneNS$_2$ with Pd^{II} and Cu^{II}

Massimiliano Arca,[a] Alexander J. Blake,[b] Vito Lippolis,*[a] Daniela R. Montesu,[a] Jonathan McMaster,[b] Lorenzo Tei,[a,b] and Martin Schröder*[b]

Keywords: Macrocycles / Palladium / Copper / N ligands / S ligands

Palladium(II) and copper(II) complexes [Pd(**L^1**)Cl$_2$], [Pd(**L^3**)Cl$_2$], [Cu(**L^1**)Cl$_2$], [Cu(**L^3**)Cl$_2$], [Pd(**L^2**)][BF$_4$]$_2$, [Pd(**L^4**)Cl]BF$_4$, [Cu(**L^2**)][NO$_3$]$_2$ and [Cu(**L^4**)Cl]PF$_6$ of the nitrile (**L^1** and **L^3**) and amino (**L^2** and **L^4**) pendant arm derivatives of 1-thia-4,7-diazacyclononane ([9]aneN$_2$S) and 7-aza-1,4-dithiacyclononane ([9]aneNS$_2$) have been prepared and fully characterised. In each case, a square-pyramidal coordination sphere is observed at both metal ions with either one or two Cl$^-$ anions completing the donor set. The tridentate nine-membered macrocyclic moiety adopts a [333] conformation in all the complexes obtained. The five-membered chelate rings involving the donor atoms of the basal plane adopt a *gauche* configuration with very similar degrees of puckering. The "innocent" nitrile pendant arms in **L^1** and **L^3** do not bind to the metal ions, but still appear to influence the binding of the tridentate macrocyclic frameworks via the tertiary amine sites.

Introduction

1,4,7-Triazacyclononane ([9]aneN$_3$) and 1,4,7-trithiacyclononane ([9]aneS$_3$; Scheme 1) have been extensively studied, and afford bis(sandwich) octahedral complexes in which the ligands bind to the metal centre in a facial manner; [9]aneN$_3$ has been used mainly to complex 3d transition metal ions[1,2] whereas the trithia analogue, [9]aneS$_3$, because of the soft nature of its donor atoms, has also been considered for complexation with 4d and 5d transition metal ions.[3] Thus, a range of complexes of noble metal ions having uncommon oxidation states have been synthesised.[3] The two related nine-membered ring macrocycles [9]aneN$_2$S (1,4-diaza-7-thiacyclononane) and [9]aneNS$_2$ (1-aza-4,7-dithiacyclononane) are of particular interest since the loss of threefold symmetry and the presence of both hard N- and soft S-donors can potentially have interesting stereochemical consequences and thereby offer specific coordination selectivity. However, their coordination chemistry has not been studied extensively,[4] perhaps in part due to the greater difficulty in preparing these mixed donor macrocycles. In comparison to [9]aneN$_3$,[5] even less attention has been directed to the *N*-functionalisation of [9]aneN$_2$S and [9]aneNS$_2$ by incorporation of pendant arms bearing coordinating donor groups to give potentially tetra- and pentadentate ligands, respectively.[4,6–13] In particular, the coordination chemistry of nitrile and amino pendant arm derivatives of [9]aneN$_2$S and [9]aneNS$_2$ such as **L^1**–**L^4** is unknown, although **L^1** and **L^2** have been described previously as free ligands.[14,15] The ethyl-bridged bis([9]aneNS$_2$), which can also be formally considered as an amino pendant arm derivative of [9]aneNS$_2$, is also known.[13] Interestingly, **L^1** and **L^4** can impose stereorestrictive modes of coordination at metal centres such as Pd^{II} and Cu^{II} by forming potentially four- or five-coordinate complexes possessing unusual and interesting coordination and/or redox properties. Due to their electronic requirements, Pd^{II} and Cu^{II} typically form square-planar and Jahn–Teller distorted octahedral complexes, respectively, and as a result, five-coordinate complexes of these metal ions would represent potential models for intermediates in associative substitution reactions at square-planar d^8 complexes, and in dissociative reactions of hexacoordinate compounds, respectively. Furthermore, five-coordinate metal complexes of coordinatively unsaturated metal centres such as Cu^{II} lead to the possibility of binding and activation of small molecules and therefore represent useful models of enzymatic systems. As a continuation of our studies[4,6–11] of the coordination chemistry of *N*-functionalised pendant arms derivatives of tridentate mixed thia/aza nine-membered macrocycles, we report herein our studies of the complexation of Pd^{II} and Cu^{II} centres with **L^1**, **L^2**, **L^3** and **L^4**.

[a] Dipartimento di Chimica Inorganica ed Analitica, Università degli Studi di Cagliari SS
554 Bivio per Sestu, 09042 Monserrato (CA), Italy
[b] School of Chemistry, The University of Nottingham, University Park, Nottingham NG7 2RD, UK

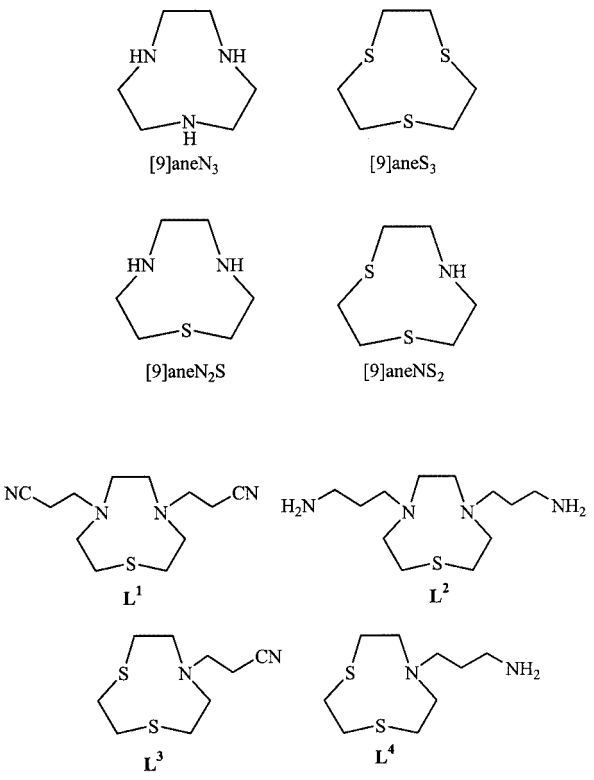

Scheme 1

Results and Discussion

Coordination to Pd^{II}

Reaction of $PdCl_2$ with 1 mol-equiv. of **L^1** in refluxing MeCN for 12 h gave an orange solution. After partial removal of the solvent and filtration through a pad of Celite, dark-red crystals of [Pd(**L^1**)Cl$_2$] were formed upon diffusion of Et_2O vapour into the remaining solution. The X-ray crystal structure of [Pd(**L^1**)Cl$_2$] (Figure 1, top; Table 1) shows a square-planar $NSCl_2$ coordination sphere at Pd^{II} with two mutually *cis*-Cl$^-$ ligands *trans* to N- and S-donors of the [9]aneN$_2$S macrocyclic framework. The remaining N-donor of the [9]aneN$_2$S ring is oriented towards the Pd^{II} centre and lies above the $NSPdCl_2$ coordination plane with a Pd···N(7) distance of 2.638(4) Å. Thus, an overall [NS+N] coordination for the [9]aneN$_2$S framework is observed. The Pd(1)−N(7) vector shows a slight deviation from perpendicularity to the Pd^{II} coordination plane with N(7)−Pd(1)−X angles [X = S(1), N(4), Cl(1) or Cl(2)] ranging from 77.23(12) to 101.23(8)°. The Pd^{II} centre lies only 0.006 Å above the mean $NSCl_2$ coordination plane and the two nitrile-functionalised pendant arms do not bind to the metal centre.

Examples of long-range Pd···N apical interactions in square-based pyramidal complexes of tridentate nine-membered macrocycles are very rare. The complex cations $[Pd([9]aneN_3)_2]^{2+}$ and $[Pd([9]aneN_3)(H[9]aneN_3)]^{3+}$ have square-planar coordination geometries at Pd^{II},[16,17] but with the remaining apical N-centres oriented away from the axial site of the PdN_4 plane at a distance of 3.499(5) Å for centrosymmetric $[Pd([9]aneN_3)_2]^{2+}$,[16] and 2.982(11)−3.079(11) Å for $[Pd([9]aneN_3)(H[9]aneN_3)]^{3+}$.[17]

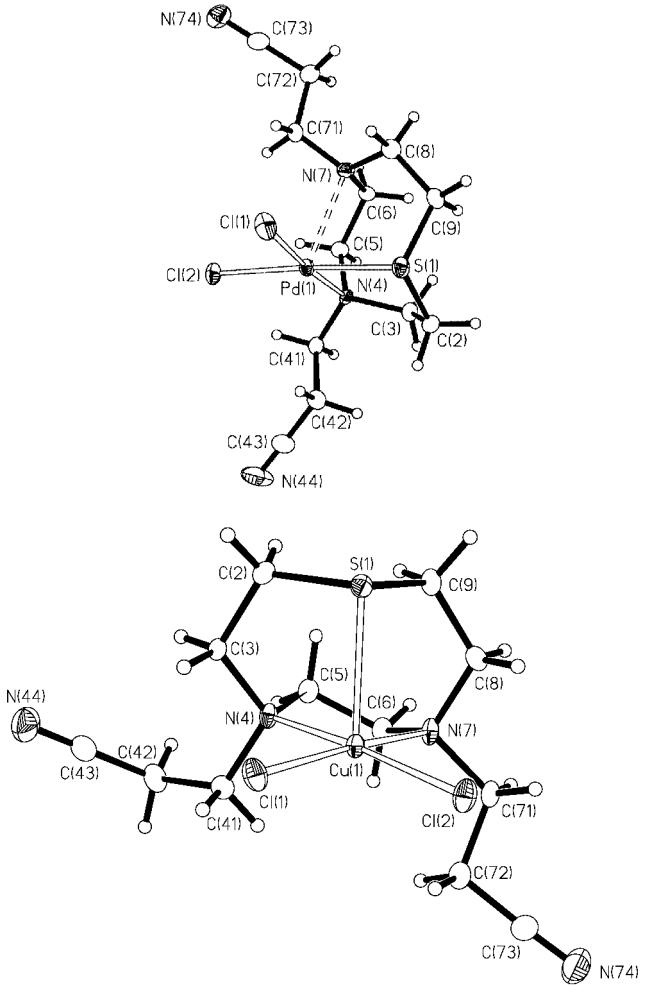

Figure 1. Structures of [Pd(**L^1**)Cl$_2$] (top) and [Cu(**L^1**)Cl$_2$] (bottom) with the numbering scheme adopted; displacement ellipsoids are drawn at 50% probability

Table 1. Selected bond lengths [Å] and angles [°] for [Pd(**L^1**)Cl$_2$] and [Cu(**L^1**)Cl$_2$]

	M = Pd	M = Cu
M(1)−S(1)	2.2492(13)	2.577(4)
M(1)−N(4)	2.124(4)	2.132(6)
M(1)−N(7)	2.638(4)	2.095(5)
M(1)−Cl(1)	2.3093(12)	2.272(2)
M(1)−Cl(2)	2.3388(12)	2.268(4)
S(1)−M(1)−N(4)	87.42(10)	82.6(2)
S(1)−M(1)−N(7)	82.02(9)	87.5(2)
S(1)−M(1)−Cl(1)	88.89(4)	97.33(11)
S(1)−M(1)−Cl(2)	176.54(4)	103.42(13)
N(4)−M(1)−N(7)	77.23(12)	83.4(2)
N(4)−M(1)−Cl(1)	175.20(10)	92.6(2)
N(4)−M(1)−Cl(2)	92.09(10)	172.4(2)
N(7)−M(1)−Cl(1)	99.23(9)	173.3(2)
N(7)−M(1)−Cl(2)	101.23(8)	92.1(2)
Cl(1)−M(1)−Cl(2)	91.79(4)	91.28(11)

Interesting exceptions are represented by the complex cation $[Pd(py_3[9]aneN_3)]^{2+}$ {$py_3[9]aneN_3$ = 1,4,7-tris(2-pyridylmethyl)-1,4,7-triazacyclononane}[2] in which one of the N-donors of the [9]aneN$_3$ framework occupies the apical site [Pd−N$_{ap}$ 2.580 Å] of a square-based pyramidal geometry. A similar geometry is observed in $[Pd(NCMe)_2(Me_3[9]aneN_3)]^{2+}$ in which the apical N-donor of the macrocycle is sited 2.523(8) from the Pd^{II} centre.[18] It is also interesting to compare the coordination modes of [9]aneN$_2$S and **L^1** to Pd^{II}. In the sandwich complexes $[Pd([9]aneN_2S)_2][PF_6]_2$ and $[Pd([9]aneN_2S)_2]Cl_2\cdot H_2O$ each metal centre is bound by four N-donors of the two macrocycles in a square-planar arrangement, with the thioether S-donors showing either long-range apical interactions with the Pd^{II} centre {as in $[Pd([9]aneN_2S)_2][PF_6]_2$} or no interaction at all {as in $[Pd([9]aneN_2S)_2]Cl_2\cdot H_2O$}.[19] A [2N+S] coordination is also observed for the [9]aneN$_2$S units in the trinuclear complex $[Pd_3([9]aneN_2S)_4Cl_2]Cl_4\cdot 2H_2O$,[19] and similar structural features have been observed for Pt^{II} complexes with both [9]aneN$_3$ and [9]aneN$_2$S[1,4,6−11] and for the complex $[Au([9]aneN_2S)Cl_2]^+$.[20] Therefore, the [NS+N] coordination of the [9]aneN$_2$S macrocyclic framework in [Pd(**L^1**)Cl$_2$] is unusual: it may have its origins in either electronic or steric effects which arise from the combination of the two nitrile functionalised pendant arms and the two bound Cl$^-$ ligands. [Pd(**L^1**)Cl$_2$] units interact with each other in the crystal lattice through long-range Cl···S contacts [3.527(2) Å] (Figure 2) to form polymeric chains of [Pd(**L^1**)Cl$_2$] which run along the (010) direction.

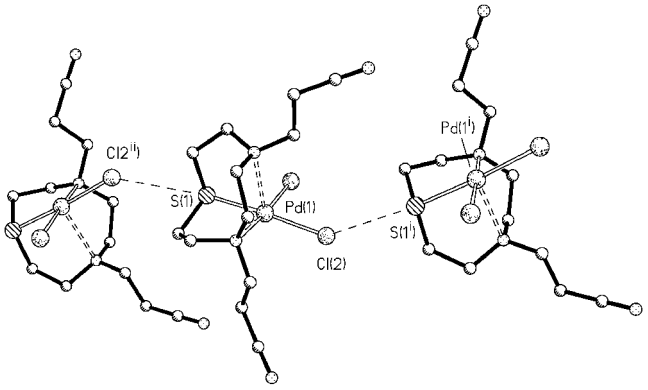

Figure 2. Partial view of the crystal packing in [Pd(**L^1**)Cl$_2$]: Cl(2)···S(1^i) 3.527(2) Å; Pd(1)−Cl(2)−S(1^i) 141.56(5), Pd(1)−S(1)−Cl(2^{ii}) 171.25(5)°; i = 1 − *x*, 1/2 + *y*, 1/2−z; ii = 1 − *x*, −1/2 + *y*, 1/2 − *z*

In order to study the effect that nitrile-functionalised pendant arms can have upon the coordination mode of mixed thia/aza nine-membered macrocyclic derivatives towards Pd^{II}, we treated **L^3** with PdCl$_2$ under the same conditions used for the synthesis of [Pd(**L^1**)Cl$_2$]. The red-orange crystals of [Pd(**L^3**)Cl$_2$] obtained after recrystallisation from DMF/Et$_2$O were analysed by X-ray diffraction. The Pd^{II} centre is bound by the two S-donors of the macrocyclic ring and two Cl$^-$ ligands to form an approximate S$_2$PdCl$_2$ plane (Figure 3, top; Table 2). The remaining tertiary N-atom of the [9]aneNS$_2$ moiety is disposed apically relative to this coordination plane with N(7)−Pd(1)−X angles [X = S(1), S(4), Cl(1) or Cl(2)] ranging from 79.24(5) to 100.94(6)°. The Pd^{II} centre is displaced 0.007 Å out of the S$_2$PdCl$_2$ mean plane in the direction of the apical N-centre. Therefore, as for [Pd(**L^1**)Cl$_2$], the addition of a nitrile pendant arm to the N-centre in [9]aneNS$_2$ leads to the macrocyclic framework adopting an unusual [2S+N] coordination in [Pd(**L^3**)Cl$_2$], with the N-centre occupying the apical position of a "flat" square-pyramidal coordination geometry. In contrast an [NS+S] coordination mode has been observed for [9]aneNS$_2$ in the complex cation $[Pd([9]aneNS_2)_2]^{2+}$ where the Pd^{II} centre is bound to two N- and two S-donors in a square-planar configuration with the remaining two S-atoms interacting apically.[21] Significantly, in the related half-sandwich complex [Pd([9]aneS$_2$O)Cl$_2$], the macrocyclic ligand assumes a facial [2S+O] coordination mode at the metal centre with the oxygen atom lying above the basal S$_2$PdCl$_2$ plane and pointing toward the Pd centre.[22] At this stage it is difficult to conclude whether the observed [NS+N] and [2S+N] coordination modes of **L^1** and **L^3** in [Pd(**L^1**)Cl$_2$] and [Pd(**L^3**)Cl$_2$], respectively, are determined by the steric requirements of the nitrile pendant arms, by electronic effects or by the binding of soft S-donors to soft Pd^{II}. It might be argued that the pendant arms in [Pd(**L^1**)Cl$_2$] and [Pd(**L^3**)Cl$_2$] tend to dispose themselves as far as possible from the Cl$^-$ ligands because of steric requirements. Alternatively, the tertiary nitrogen centres in **L^1** and **L^3** may have a weaker σ-donor character than the analogous secondary N-donors in [9]aneN$_2$S and [9]aneNS$_2$. According to molecular orbital calculations performed by Rossi and Hoffmann for d^8 low-spin metal centres,[23] this would lead to a tendency for the N-donor to lie in the apical position of a square-based pyramidal coordination geometry. However, thioether donors in macrocyclic systems have a limited π-donor/acceptor capacity,[3] and according to calculations performed by Rossi and Hoffmann for a five-coordinate, square-based pyramidal geometry, the disposition and the relative bond strengths of the substituents in the apical and basal positions, as well as the degree of pyramidality, are the result of a delicate balance between σ- and π-substituent effects.[23]

In both [Pd(**L^1**)Cl$_2$] and [Pd(**L^3**)Cl$_2$] the nitrile groups of the pendant arms are directed away from the metal centre. We argued that conversion of nitriles to amine functions would switch the coordination mode at Pd^{II} and restore the more usual [2N+S] and [NS+S] binding of the [9]aneN$_2$S and [9]aneNS$_2$ moieties in **L^2** and **L^4**, respectively. This would be driven by the formation of six-membered chelate rings on coordination of the strongly donating amine pendant arms to Pd^{II}. The reaction of **L^2** with 1 mol-equiv. of $[Pd(CH_3CN)_4](BF_4)_2$ in MeCN/MeOH at room temperature yielded a yellow solid after removal of the solvent. Recrystallisation by diffusion of Et$_2$O into a solution of the complex in MeNO$_2$ afforded pale-yellow crystals which, according to analytical and mass spectrometric data, had the formulation [Pd(**L^2**)][BF$_4$]$_2$. A crystal structure determination confirmed the formation of the cation [Pd(**L^2**)]$^{2+}$ (Figure 4, top; Table 3), with the pentadentate ligand **L^2** impos-

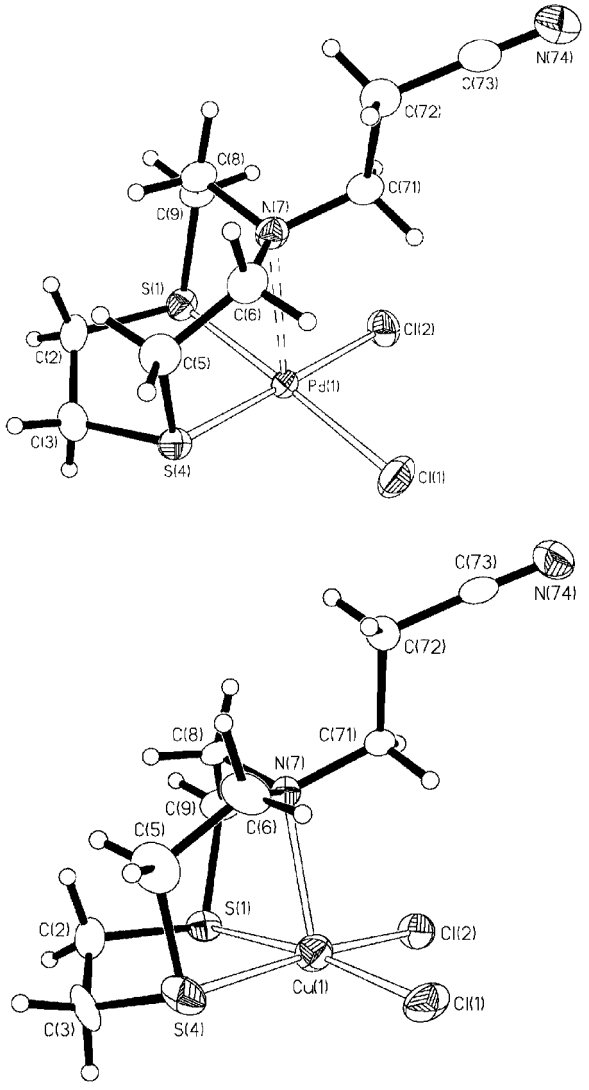

Figure 3. Structures of [Pd(**L^3**)Cl$_2$] (top) and [Cu(**L^3**)Cl$_2$] (bottom) with the numbering scheme adopted; displacement ellipsoids are drawn at 50% probability

Table 2. Selected bond lengths [Å] and angles [°] for [Pd(**L^3**)Cl$_2$] and [Cu(**L^3**)Cl$_2$]

	M = Pd	M = Cu
M(1)−S(1)	2.2685(8)	2.313(2)
M(1)−S(4)	2.2532(9)	2.340(2)
M(1)−N(7)	2.722(2)	2.333(4)
M(1)−Cl(1)	2.3282(9)	2.256(2)
M(1)−Cl(2)	2.3258(9)	2.277(2)
S(1)−M(1)−S(4)	89.76(3)	87.40(6)
S(1)−M(1)−N(7)	79.24(5)	85.34(10)
S(1)−M(1)−Cl(1)	177.90(3)	172.70(6)
S(1)−M(1)−Cl(2)	89.29(3)	86.90(6)
S(4)−M(1)−N(7)	81.31(6)	85.38(10)
S(4)−M(1)−Cl(1)	88.20(3)	88.37(6)
S(4)−M(1)−Cl(2)	179.03(3)	171.18(7)
N(7)−M(1)−Cl(1)	100.94(6)	100.25(10)
N(7)−M(1)−Cl(2)	98.70(6)	100.85(10)
Cl(1)−M(1)−Cl(2)	92.74(3)	

ing a formal [4+1] coordination sphere at the Pd^{II} centre, which is bound by the two tertiary N-donors of the [9]aneN$_2$S ring and the nitrogen atoms of both amino pendant arms forming an approximate PdN$_4$ plane. The S-donor of the macrocyclic ring occupies an apical site of a distorted square-pyramidal geometry with a long-range Pd···S(1) interaction of 3.0865(11) Å. The Pd^{II} centre is displaced 0.07 Å out of the mean plane defined by the atoms N(4), N(7), N(44) and N(74) towards S(1), with the angles S(1)−Pd(1)−N$_{eq}$ ranging from 75.60(9) to 106.72(9)°. Therefore, the introduction of coordinating functionalised pendant arms does indeed switch the [9]aneN$_2$S moiety of **L^2** to adopt a facial [2N+S] donation to Pd^{II} rather than the [NS+N] mode observed for **L^1** in [Pd(**L^1**)Cl$_2$] (see above). The Pd···S(1) distance in [Pd(**L^2**)]$^{2+}$ is consistent with those for long-range Pd···S apical interactions found in other sandwich and half-sandwich Pd^{II} complexes with thia- and mixed thia/aza macrocycles.[3,19−21,24−32] In [Pd(**L^2**)]$^{2+}$ (Figure 4, top) there are one five- and two six-membered chelate rings involving the metal centre. The former adopts a *gauche* conformation with a torsion angle at the C(5)−C(6) bond of 45.7(5)°, while the latter adopt chair forms. The chelate angles range from 86.47(13) [N(4)−Pd(1)−N(7)] to 93.02(14)° [N(4)−Pd(1)−N(44)] and do not suggest any particular structural or steric constraints imposed by the five- and six-membered chelate rings.

Reaction of [Pd(CH$_3$CN)$_4$](BF$_4$)$_2$ with **L^4** affords a brown oil which was treated with 1 mol-equiv. of aqueous NaCl at room temperature to give, after removal of the solvent, a brown solid which could be recrystallised from MeCN/Et$_2$O. The fast-atom bombardment (FAB) mass spectrum of the product exhibited peaks with the correct isotopic distribution for [^{106}PdCl(**L^4**)]$^+$ (*m*/*z* = 362) and for [^{106}Pd(**L^4**)]$^+$ (*m*/*z* = 327). These, together with elemental analytical data, suggest a formulation [Pd(**L^4**)Cl]BF$_4$. An X-ray diffraction study confirmed the formation of the complex cation [Pd(**L^4**)Cl]$^+$ in which a formal [4+1] square-based pyramidal geometry is achieved at the metal centre (Figure 5, top; Table 4). One N- and one S-donor of the macrocyclic framework, the amino group of the pendant arm and one Cl$^-$ ligand are coordinated to the Pd^{II} centre in a square-planar arrangement. The remaining S-donor of [9]aneNS$_2$ shows a long-range apical Pd···S(4) interaction of 2.9278(9) Å, with the metal atom displaced only 0.004 Å out of the N$_2$SCl mean plane towards S(4). Symmetry-related [Pd(**L^4**)Cl]$^+$ complex cations interact with each other to form dimeric units through Pd···Cl contacts of 3.6091(11) Å, while the S-donors in the PdN$_2$SCl coordination plane interact with F$^-$ centres in BF$_4^-$ counter-anions (Figure 6, top).

Significantly, the Pd···S$_{ap}$ interaction in [Pd(**L^4**)Cl]$^+$ is shorter than that observed in the sandwich complex cation [Pd([9]aneNS$_2$)$_2$]$^{2+}$ [3.011(3) Å],[21] even though the overall cationic charge of the former is lower. This demonstrates once again that apical interactions in square-pyramidal Pd^{II} and Pt^{II} complexes are influenced significantly by the electronic nature of the equatorial ligands. As predicted, the binding of **L^2** and **L^4** to Pd^{II} drives the [9]aneN$_2$S and

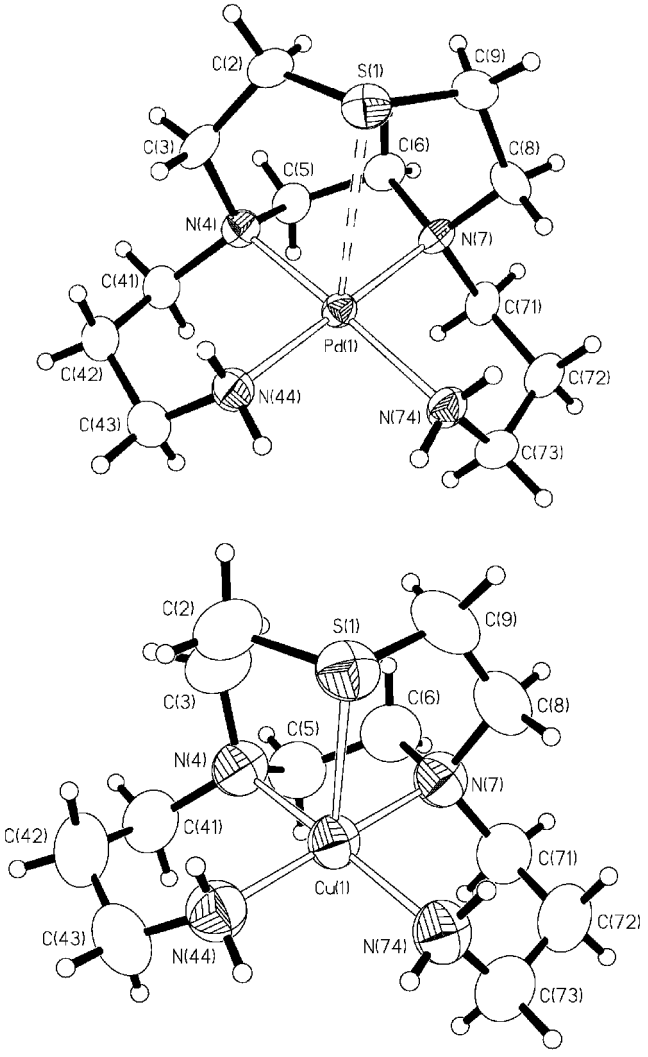

Figure 4. Structures of the complex cations $[Pd(\mathbf{L^2})]^{2+}$ (top) and $[Cu(\mathbf{L^2})]^{2+}$ (bottom) with the numbering scheme adopted; displacement ellipsoids are drawn at 50% probability

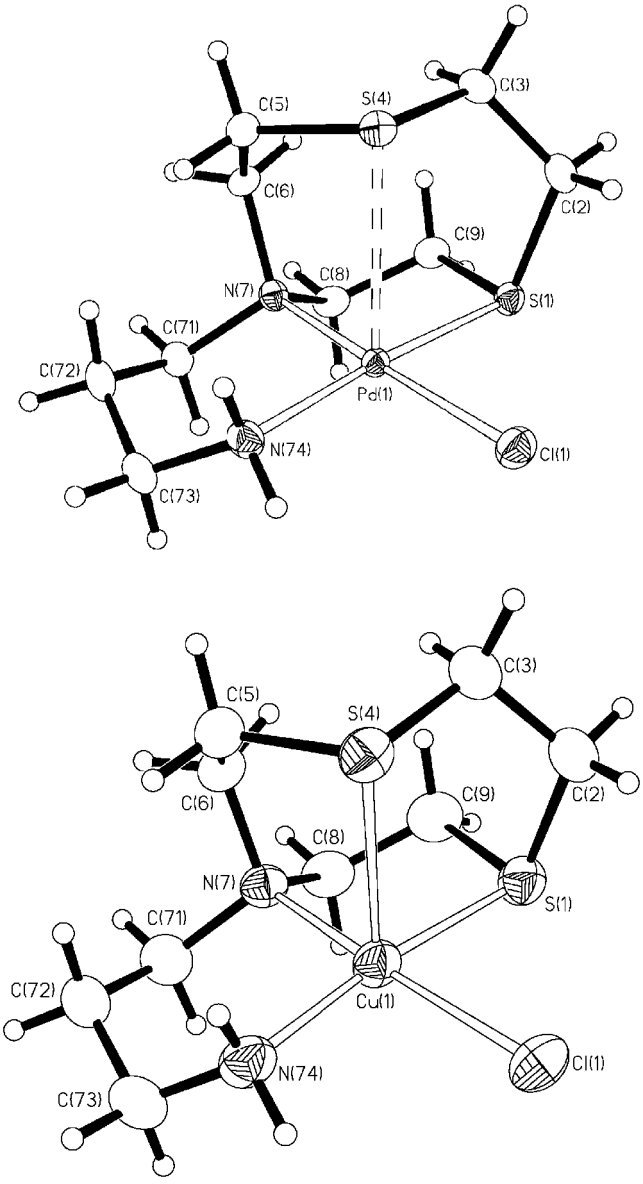

Figure 5. Structures of the complex cations $[Pd(\mathbf{L^4})Cl]^{+}$ (top) and $[Cu(\mathbf{L^4})Cl]^{+}$ (bottom) with the numbering scheme adopted; displacement ellipsoids are drawn at 50% probability

Table 3. Selected bond lengths [Å] and angles [°] for $[Pd(\mathbf{L^2})][BF_4]_2$ and $[Cu(\mathbf{L^2})][NO_3]_2$

	M = Pd	M = Cu
M(1)−S(1)	3.0865(11)	2.5608(13)
M(1)−N(4)	2.075(4)	2.070(4)
M(1)−N(7)	2.077(3)	2.093(4)
M(1)−N(44)	2.052(3)	2.025(4)
M(1)−N(74)	2.064(3)	2.013(4)
S(1)−M(1)−N(4)	80.19(10)	88.07(11)
S(1)−M(1)−N(7)	75.60(9)	85.80(11)
S(1)−M(1)−N(44)	104.80(10)	96.61(13)
S(1)−M(1)−N(74)	106.72(9)	99.71(12)
N(4)−M(1)−N(7)	86.47(13)	84.5(2)
N(4)−M(1)−N(44)	93.02(14)	93.6(2)
N(4)−M(1)−N(74)	172.14(14)	170.6(2)
N(7)−M(1)−N(44)	179.29(13)	176.8(2)
N(7)−M(1)−N(74)	91.60(12)	90.8(2)
N(44)−M(1)−N(74)	88.84(14)	90.8(2)

[9]aneNS$_2$ moieties to bind facially with long-range S-donor apical interactions as opposed to long-range N-donor interactions in the case of $\mathbf{L^1}$ and $\mathbf{L^2}$.

While the macrocyclic ligands in $[Pd([9]aneN_3)_2]^{2+}$,[16] half-sandwich Pd^{II} complexes with [9]aneS$_3$[25] and $[Pt([9]aneS_3)phen]^{2+}$[32] have been shown to be fluxional in solution, no evidence of similar behaviour has yet been reported for mixed thia/aza macrocycles [9]aneN$_2$S and [9]aneNS$_2$ or their derivatives. For $[Pd(py_2[9]aneN_2S)]^{2+}$ it has been shown by NMR spectroscopy that the ligand is nonfluxional in solution, with the axial S-donor believed to maintain a constant position by weak interaction with the Pd^{II} centre.[26] The structures of $[Pd(\mathbf{L^1})Cl_2]$ and $[Pd(\mathbf{L^3})Cl_2]$ clearly demonstrate the possibility for [9]aneN$_2$S, [9]aneNS$_2$ and their derivatives to adopt different facial coordination

Table 4. Selected bond lengths [Å] and angles [°] for [Pd(**L**^{4})Cl]BF$_4$ and [Cu(**L**^{4})Cl]PF$_6$

	M = Pd	M = Cu
M(1)−S(1)	2.2633(8)	2.2938(11)
M(1)−S(4)	2.9278(9)	2.5962(11)
M(1)−N(7)	2.087(2)	2.103(3)
M(1)−N(74)	2.077(2)	1.996(3)
M(1)−Cl(1)	2.3381(9)	2.3567(11)
S(1)−M(1)−S(4)	84.00(3)	87.91(4)
S(1)−M(1)−N(7)	87.04(6)	87.01(9)
S(1)−M(1)−N(74)	175.91(7)	173.49(11)
S(1)−M(1)−Cl(1)	89.37(3)	86.76(4)
S(4)−M(1)−N(7)	84.56(6)	87.52(9)
S(4)−M(1)−N(74)	99.19(7)	97.87(11)
S(4)−M(1)−Cl(1)	96.26(3)	95.89(4)
N(7)−M(1)−N(74)	95.79(9)	96.20(13)
N(7)−M(1)−Cl(1)	176.21(6)	172.78(9)
N(74)−M(1)−Cl(1)	87.74(7)	89.65(10)

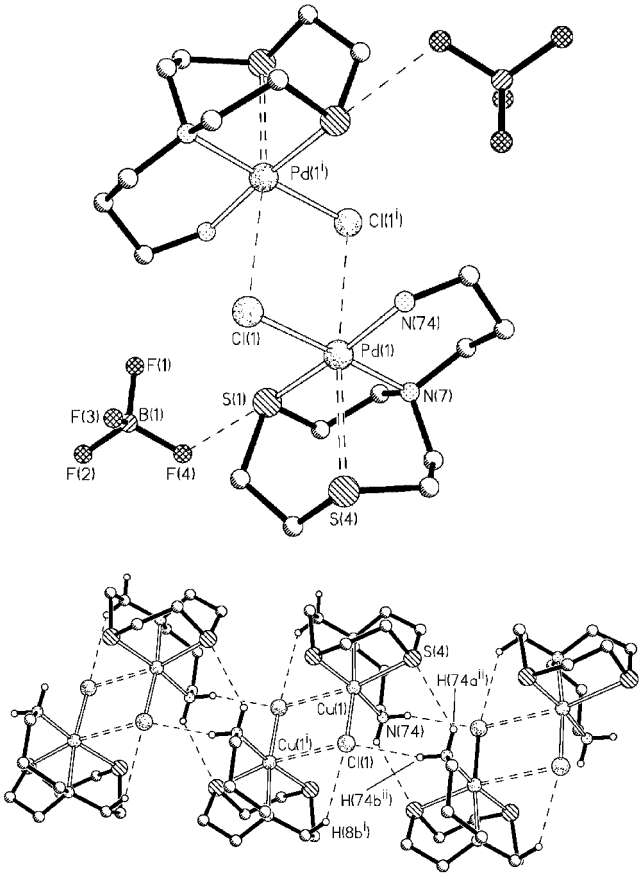

Figure 6. Top: dimeric units of [Pd(**L**^{4})Cl]$^+$ complex cations interacting with BF_4^- anions [Pd···Cl(1^i) 3.6091(11) Å; Cl(1^i)···Pd(1)−S(4) 167.13(2), Pd(1)−Cl(1)···Pd(1^i) 84.55(2)°; S(1)···F(4) 3.179(2) Å; F(4)···S(1)−Pd(1) 173.51(5)°; i = 1 − *x*, 2 − *y*, 1 − *z*]; bottom: view of part of an infinite ribbon of [Cu(**L**^{4})Cl]$^+$ cations running along the (100) direction; only those H atoms which are involved in hydrogen bonding are shown [Cu(1^i)···Cl(1) 3.1514(12), Cl(1)···H(8b^i) 2.801, Cl(1)···H(74b^{ii}) 2.656, S(4)···H(74a^{ii}) 2.903 Å; Cu(1)−Cl(1)···H(8b^i) 141.8°; i = − *x*, 2 − *y*, 1 − *z*; ii = 1 − *x*, 2 − *y*, 1 − *z*]

modes at low-spin d^8 metal centres. Furthermore, the structure of [Pd([9]aneN$_2$S)$_2$]Cl$_2$·H$_2$O shows that the S-centres do not interact apically with the metal centre[19] and this situation could represent the first step towards a dynamic structure in solution in which the metal atom undergoes a series of inner-sphere substitution reactions with the ligand rotating between [2N+S] and [NS+N] configurations. Although the results herein apply only to situations in the solid state, they confirm the low energy differences between these different possible coordination modes and suggest that fluxional behaviour in solution may be possible for [9]aneN$_2$S and [9]aneNS$_2$ within sandwich and half-sandwich complexes with Pd^{II} and Pt^{II}. Unfortunately, due to the very low solubilities of [Pd(**L**^{1})Cl$_2$] and [Pd(**L**^{3})Cl$_2$] we have not been able to demonstrate this in solution.

Coordination to Cu^{II}

Reaction of **L**^{1} with 1 mol-equiv. of CuCl$_2$·2H$_2$O in MeCN afforded a green solution after 1 h of reflux under N$_2$. Slow concentration of this solution yielded green crystals having the formulation [Cu(**L**^{1})Cl$_2$] according to analytical and mass spectrometric data. A crystal structure determination (Figure 1, bottom; Table 1) shows the metal centre in a distorted square-pyramidal environment, with the basal positions occupied by the two tertiary N-donors of the [9]aneN$_2$S moiety of **L**^{1} and by two Cl$^-$ ligands. The S-donor S(1) of the macrocyclic ring occupies the apical position whereas the nitrile functionalised pendant arms are directed away from the metal centre. The Cu^{II} centre is displaced 0.1145 Å out of the mean plane defined by the atoms N(4), N(7), Cl(1) and Cl(2), in the direction of S(1). The structure of [Cu(**L**^{1})Cl$_2$] is very similar to that reported for the half-sandwich complex [Cu([9]aneN$_2$S)Br$_2$],[33] where the macrocyclic ligand also adopts a facial [2N+S] coordination at the metal centre [Cu−N$_{eq}$ 2.03(1), 2.02(1) Å; Cu−S$_{ap}$ 2.567(3) Å] but with two Br$^-$ ligands at basal positions completing the square-pyramidal geometry. However, the Cu−N$_{eq}$ distances appear significantly longer in the case of [Cu(**L**^{1})Cl$_2$] (Table 1) and this could be due to an increased steric repulsion at the tertiary N-centres in **L**^{1} compared to the secondary N-centres in [9]aneN$_2$S. Cu−S$_{ap}$ bonds longer than those reported for [Cu([9]aneN$_2$S)Br$_2$][33] and [Cu(**L**^{1})Cl$_2$] have been observed for the sandwich complex [Cu([9]aneN$_2$S)$_2$]$^{2+}$ [Cu−N$_{eq}$ 2.027(3), 2.067(3); Cu−S$_{ap}$ 2.707(1) Å] in which the macrocyclic ligand also adopts a facial [2N+S] coordination mode.[34,35] [Cu(**L**^{1})Cl$_2$] provides an interesting contrast to [Pd(**L**^{1})Cl$_2$] in that changing the metal centre from low-spin d^8 to d^9 causes the [9]aneN$_2$S framework of **L**^{1} to pass from the [NS+S] to the [2N+S] facial coordination mode. This is clearly consistent with the preference of Cu^{II} for binding N-donor centres, as also demonstrated by the structure of the sandwich complex [Cu([9]aneN$_2$S)$_2$]$^{2+}$ in which the four N-donors occupy the equatorial sites of a distorted octahedral geometry and the two S-donors occupy the axial positions.[33,34]

In order to investigate the coordinative behaviour of the [9]aneNS$_2$ moiety in **L**^{3} towards Cu^{II}, **L**^{3} was treated with

1 mol-equiv. of $CuCl_2 \cdot 2H_2O$ in MeCN under the same experimental conditions used for the synthesis of $[Cu(\mathbf{L^1})Cl_2]$. Well-shaped crystals of $[Cu(\mathbf{L^3})Cl_2]$ suitable for X-ray diffraction studies were obtained after recrystallisation from DMF/Et_2O. The [2S+N] ligand arrangement in $[Cu(\mathbf{L^3})Cl_2]$ (Figure 3, bottom; Table 2) is very similar to that observed in $[Pd(\mathbf{L^3})Cl_2]$ but contrasts with that observed for $[Cu(\mathbf{L^1})Cl_2]$. In $[Cu(\mathbf{L^3})Cl_2]$ it appears that the preference of Cu^{II} for N-donors is offset by steric effects of the bulky tertiary N-donors which induces the [9]aneNS$_2$ framework to adopt the observed [2S + N] coordination mode. A similar coordination mode is observed in $[Cu([9]aneNS_2)_2]^{2+}$ with the S-donors occupying the equatorial sites of an octahedral geometry [Cu−S_{eq} 2.547(1)−2.539(1) Å] and the N-donors at the axial positions average [Cu−N_{eq} 2.016(4) Å].[36] In this case the average Cu−N_{eq} distance is much shorter and the Cu−S_{eq} are much longer than the corresponding bond lengths observed in $[Cu(\mathbf{L^3})Cl_2]$ suggesting a possible opposite direction of the Jahn−Teller effect in the two complexes. It appears, therefore, that a delicate balance between electronic and steric factors might be responsible for the type of donation of the macrocyclic framework in the square-pyramidal complexes $[M(\mathbf{L^1})Cl_2]$ and $[M(\mathbf{L^3})Cl_2]$ (M = Pd, Cu).

$[Cu(\mathbf{L^3})Cl_2]$ units in the crystal lattice interact with each other via long Cl···Cu contacts to give infinite zigzag chains which run along the *c* axis, with the nitrile-functionalised pendant arms dangling away from the metal centres (Figure 7).

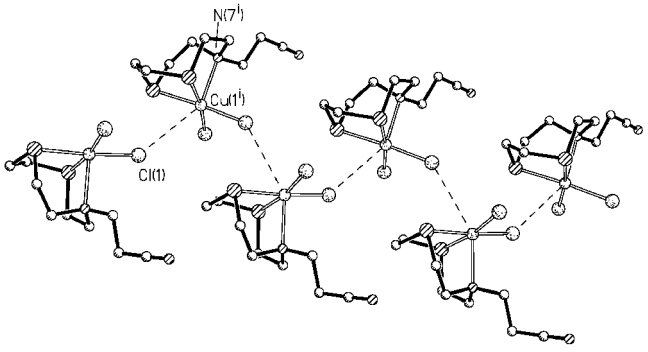

Figure 7. Partial view along the (110) direction of zigzag chains of $[Cu(\mathbf{L^3})Cl_2]$ molecules running along the (001) direction: Cl(1)···Cu(1^{i}) 3.5886(11) Å; Cl(1)···Cu(1^{i})−N(7^{i}) 150.52(10)°; i = 1 − *x*, − *y*, *z* − 1/2

Given that structural data on CuN_4S systems are relatively rare in the literature, we treated $\mathbf{L^2}$ with 1 mol-equiv. of $Cu(NO_3)_2 \cdot 3H_2O$ in MeCN/EtOH at room temperature. A blue colour was immediately formed and the residue obtained after removal of the solvent was repeatedly crystallised from EtOH/Et_2O to give blue blocky crystals having the formulation $[Cu(\mathbf{L^2})][NO_3]_2$.

As observed for $[Pd(\mathbf{L^2})]^{2+}$, the structure of the cation $[Cu(\mathbf{L^2})]^{2+}$ (Figure 4, bottom; Table 3) shows the ligand encapsulating the metal ion in a distorted square-based pyramidal geometry. The basal coordination sites are occupied by the N-atoms of the [9]aneN$_2$S moiety and by the primary amino groups of the pendant arms, with the remaining S-donor of the pentadentate ligand $\mathbf{L^2}$ occupying the apical position. The metal ion is displaced out of the N_4 plane by 0.0965 Å in the direction of the S donor. The Cu−N_{eq} bond lengths [average 2.05(2) Å] are typical for an N_4-donor set arranged in a plane around the Cu^{II} centre, and similar average Cu−N_{eq} bond lengths have been observed for Cu^{II} complexes of amino-functionalised pendant arm derivatives of [9]aneN$_3$ and ethyl-bridged bis([9]aneN$_3$).[37] The Cu−S_{ap} bond length [2.5608(13) Å] is towards the lower end of the range [2.56−2.82 Å] expected for axial Cu−S contacts.[34] The structure of $[Cu(\mathbf{L^2})]^{2+}$ can be compared to those of $[Cu(py_2[9]aneN_2S)]^{2+}$ [Cu−S_{ap} = 2.496(8), Cu−N_{eq} = 2.02(1) Å][38] and [Cu(*b*[10.5.2][19]aneN$_4$S)]$^{2+}$ bicyclo [Cu−S_{ap} = 2.549(2), Cu−N_{eq} = 2.04(1) Å][14] {py$_2$[9]aneN$_2$S = 4,7-bis(2-pyridylmethyl)-1-thia-4,7-diazacyclononane; *b*[10.5.2][19]aneN$_4$S = 15-thia-1,5,8,12-tetraazabicyclo[10.5.2]nonadecane}. These represent the only examples of structurally characterised CuN_4S systems with a square-pyramidal coordination sphere at the metal centre. Py$_2$[9]aneN$_2$S differs from $\mathbf{L^2}$ in that it has pyridyl-functionalised pendant arms, whereas *b*[10.5.2][19]aneN$_4$S can be considered as derived from $\mathbf{L^2}$ by formally joining the primary amino groups of the pendant arms with a $-CH_2CH_2-$ bridge to form a tetraazamacrocycle fused with a [9]aneN$_2$S moiety. In the case of $[Cu(py_2[9]aneN_2S)]^{2+}$, the structural data seem to indicate the presence of significant geometric constraints imposed by the pentadentate ligand py$_2$[9]aneN$_2$S. Indeed, the Cu−S_{ap} bond is particularly short and, although the mean Cu−N_{eq} bond length is similar for all three complexes, the Cu−N_{eq} bonds involving the pyridine donors in $[Cu(py_2[9]aneN_2S)]^{2+}$ are significantly shorter.[14,38] A similar trend in M−S_{ap} and M−N_{eq} distances is observed when comparing $[Pd(\mathbf{L^2})]^{2+}$ with $[Pd(py_2[9]aneN_2S)]^{2+}$.[26] Finally, the rather strained square-pyramidal coordination imposed on Cu^{II} by py$_2$[9]aneN$_2$S is also seen in the strong distortion of the basal plane in $[Cu(py_2[9]aneN_2S)]^{2+}$ where the metal centre suffers by far the greatest displacement (0.22 Å) from the N_4 plane towards the apical S-donor in the three complexes considered.

The ligand $\mathbf{L^4}$ was treated with 1 mol-equiv. of $CuCl_2 \cdot 2H_2O$ in MeOH at room temperature to give a deep blue solution. Addition of excess NH_4PF_6 followed by removal of the solvent gave a blue product, which was recrystallised from MeCN/Et_2O. The fast-atom bombardment (FAB) mass spectrum of this product exhibits peaks with the correct isotopic distribution for $[^{63}Cu(\mathbf{L^4})Cl]^+$ (*m*/*z* = 319) and for $[^{63}Cu(\mathbf{L^4})]^+$ (*m*/*z* = 284), and elemental analytical data suggested a formulation $[Cu(\mathbf{L^4})Cl]PF_6$. A structure determination confirmed the formation of a $[Cu(\mathbf{L^4})Cl]^+$ cation (Figure 5, bottom; Table 4) having structural features very similar to those observed in the analogous Pd^{II} complex $[Pd(\mathbf{L^4}Cl)]^+$. The square-pyramidal coordination geometry in $[Cu(\mathbf{L^4})Cl)]^+$ involves an N_2SCl donor set defining the basal plane and an S-donor at the apical site. The Cu−S_{ap} bond length is 2.5962(11) Å and, as expected, the Cu−N_{eq} distance involving the amino pen-

dant arm group [1.996(3) Å] is shorter than that involving the tertiary N-donor of the macrocyclic ring [2.103(3) Å]. The metal centre is displaced 0.1307 Å out of the mean plane defined by the atoms N(74), N(7), S(1) and Cl(1) in the direction of the apical S-donor S(4). In [Cu(**L^4**)Cl]$^+$, as in [Pd(**L^4**)Cl]$^+$, the coordination of the amino pendant arm to the metal centre with the formation of a six-membered chelate ring has driven the [9]aneNS$_2$ framework to adopt a facial [NS+S] coordination mode in contrast to the [2N+S] binding observed in [Cu(**L^2**)Cl$_2$] and [Pd(**L^2**)Cl$_2$]. [Cu(**L^4**)Cl]$^+$ units are associated in pairs via long-range Cu···Cl contacts and Cl···H hydrogen bonds, giving a Cu···Cu distance of 4.001(1) Å (Figure 6, bottom). Also, pairs of [Cu(**L^4**)Cl]$^+$ cations interact with each other through hydrogen bonds involving the amino pendant arm of the ligand to give ribbons which run along the *a* axis.

Conclusions

The binding of **L^1**−**L^4** to Pd^{II} and Cu^{II} is the same for each pair of complexes (Table 5) except for [M(**L^1**)Cl$_2$] for which both [NS+N] (M = Pd) and [2N + S] (M = Cu) coordination modes are observed. Generally, the amine ligands **L^2** and **L^4** show strong basal coordination of the N-donors of the macrocycle and of the primary amine. This is driven by the excellent binding properties of the primary amine donors and by the inherent stability of the chelate rings thus formed. The apparently "innocent" nitrile pendant arms are found to modulate the binding of the macrocyclic units within complexes of **L^1** and **L^3** and afford rare examples of long-range apical Pd···N$_{ap}$ interactions.

Experimental Section

General: Melting points are uncorrected. Microanalyses were performed by the University of Nottingham School of Chemistry Microanalytical Service. IR spectra were recorded as KBr discs using a Perkin−Elmer 598 spectrometer over the range 400−4000 cm^{-1}. NMR spectra (^{1}H and ^{13}C) were recorded at 298 K with a Bruker DPX300 instrument. UV/Vis spectra were measured in quartz cells using a Perkin−Elmer Lambda 9 spectrophotometer. Reagents and analytical-grade materials were obtained from commercial suppliers and used without further purification. All solvents were dried by conventional methods, freshly distilled and degassed. All reactions of air- and water-sensitive materials were performed in oven-dried glassware under dinitrogen. **L^1**,[14,39,40] **L^2** [14] and **L^3** [39,40] were synthesised according to literature procedures.

Table 5. Summary of coordination modes in Pd^{II} and Cu^{II} complexes of **L^1**−**L^4**

	M = Pd	M = Cu
[M(**L^1**)Cl$_2$]	[NS + N]	[2N + S]
[M(**L^2**)]$^{2+}$	[2N + S]	[2N + S]
[M(**L^3**)Cl$_2$]	[2S + N]	[2S + N]
[M(**L^4**)Cl]$^+$	[NS + S]	[NS + S]

Synthesis of L^4: A mixture of **L^3** (0.879 g, 3.99 × 10^{-3} mol) and BH$_3$·THF (1 M THF solution, 25 mL) was refluxed under N$_2$ for 48 h. The mixture was cooled and water (40 mL) was slowly added to destroy excess BH$_3$. The solvent was removed in vacuo and the solid residue was treated with 2 M HCl (50 mL) under reflux for 2 h. The solvent was removed under reduced pressure and the residue dried in vacuo. The white solid obtained was dissolved in water and the solution passed through an ion-exchange resin (Dowex 1X8-200) to give, after removal of the solvent, a colourless oil (0.585 g, 65% yield). EI$^+$ MS: *m*/*z* = 161 [M$^+$ − CH$_2$CH$_2$S], 147 [M$^+$ − CH$_2$ − CH$_2$CH$_2$S]. ^{1}H NMR (CDCl$_3$, 300 MHz): δ = 1.52 (quint, *J* = 7.23 Hz, 2 H, NCH$_2$*C*H$_2$CH$_2$NH$_2$), 2.43−2.81 (m, 12 H, NC*H*$_2$CH$_2$C*H*$_2$NH$_2$, NC*H*$_2$C*H*$_2$S), 3.06 (s, 4 H, SC*H*$_2$C*H*$_2$S) ppm. ^{13}C NMR (CDCl$_3$, 75.47 MHz): δ = 31.2, 32.6 (*C*H$_2$S*C*H$_2$), 34.2 (NCH$_2$*C*H$_2$CH$_2$NH$_2$), 39.8 (NCH$_2$CH$_2$*C*H$_2$NH$_2$), 54.7 (N*C*H$_2$CH$_2$CH$_2$NH$_2$), 57.7 (N*C*H$_2$CH$_2$S) ppm. IR spectrum (film between KCl discs): ṽ = 3277 br. m, 2911 s, 2800 s, 1627 m, 1572 m, 1461 m, 1405 m, 1305 m, 1144 w, 1111 w, 1022 w, 905 w, 811 w cm^{-1}.

[Pd(L^1)Cl$_2$]: A mixture of **L^1** (30 mg, 0.12 mmol) and PdCl$_2$ (21.08 mg, 0.12 mmol) in MeCN (10 mL) was refluxed overnight under N$_2$. The solvent was partially removed under reduced pressure and the resulting orange solution was filtered. Et$_2$O vapour was allowed to diffuse into the filtrate solution giving 37 mg (72% yield) of dark red microcrystals. Diffraction-quality crystals were obtained by recrystallisation from MeCN/Et$_2$O. M.p. 200−204 °C (dec.).C$_{12}$H$_{20}$Cl$_2$N$_4$PdS (429.68): calcd. C 33.54, H 4.69, N 13.04; found C 33.32, H 4.13, N 12.88. ES$^+$ MS: *m*/*z* = 427; calcd. for [^{106}Pd(**L^1**)Cl$_2$]$^+$ [M$^+$] 428. UV/Vis (MeCN): λ$_{max}$ (ε$_{max}$) = 400 nm (606 dm^3 mol^{-1} cm^{-1}). IR (KBr disc): ṽ = 2926 m, 2875 w, 2823 w, 2242 s, 1478 m, 1456 s, 1412 m, 1356 m, 1286 m, 1236 w, 1207 m, 1187 w, 1126 m, 1094 m, 1008 m, 931 m, 940 w, 908 w, 860 w, 760 m, 586 w cm^{-1}.

[Pd(L^3)Cl$_2$]: A mixture of **L^3** (20 mg, 0.092 mmol) and PdCl$_2$ (16.31 mg, 0.092 mmol) in MeCN (10 mL) was refluxed overnight under N$_2$. The resulting solution was filtered through a pad of Celite and the solvent removed under reduced pressure to give a red-brown residue. Recrystallisation by diffusion of Et$_2$O vapour into a DMF solution of the obtained solid gave red-orange crystals (20 mg, 55% yield). M.p. 260−262 °C (dec.). C$_9$H$_{16}$Cl$_2$N$_2$PdS$_2$ (393.66): calcd. C 27.46, H 4.10, N 7.12; found C 26.98 , H 3.88, N 6.90. FAB MS [3-nitrobenzyl alcohol(3-noba)]: *m*/*z* = 359; calcd. for [^{106}PdCl(**L^3**)]$^+$ [M$^+$] 358. UV/Vis (DMF): λ$_{max}$ (ε$_{max}$) = 410 nm (945 dm^3 mol^{-1} cm^{-1}). IR spectrum (KBr disc): ṽ = 2978 m, 2950 m, 2827 m, 2246 m, 1453 m, 1440 m, 1400 s, 1371 m, 1346 s, 1298 m, 1132 m, 1113 m, 1045 w, 1011 m, 959 m, 926 m, 896 w, 808 w, 736 w, 654 w, 580 w cm^{-1}.

[Pd(L^2)][BF$_4$]$_2$: A mixture of **L^2** (50 mg, 0.1920 mmol) and Pd(CH$_3$CN)$_4$(BF$_4$)$_2$ (85.3 mg, 0.1920 mmol) in MeCN/MeOH (1:1, v/v; 10 mL) was stirred at room temperature for 4 h. The solvent was removed in vacuo to give a yellow solid. Diffusion of Et$_2$O vapour into a solution of the complex in MeNO$_2$ afforded pale yellow crystals (77.5 mg, 75% yield). M.p. 214−216 °C. C$_{12}$H$_{28}$B$_2$F$_8$N$_4$PdS (540.46): calcd. C 26.67, H 5.22, N 10.37; found C 27.09, H 5.53, N 10.77. FAB MS (3-noba): *m*/*z* = 453, 366; calcd. for [^{106}Pd(**L^2**)(BF$_4$)]$^+$ [M$^+$] 454 and [^{106}Pd(**L^2**)]$^+$ [M$^+$] 367. UV/Vis (MeCN): λ$_{max}$ (ε$_{max}$) = 300 (459), 396 nm (60 dm^3 mol^{-1} cm^{-1}). IR (KBr disc): ṽ = 3310 s, 3276 s, 3171 m, 3096 m, 2944 m, 1612 s, 1469 m, 1328 m, 1175 s, 1087 s, 992 s, 771 m, 540 m, 420 w cm^{-1}.

[Pd(L^4)Cl]BF$_4$: A mixture of **L^4** (21 mg, 0.0953 mmol) and Pd(CH$_3$CN)$_4$(BF$_4$)$_2$ (42.33 mg, 0.0953 mmol) in MeCN (5 mL) was

stirred at room temperature for 48 h. The solvent was removed in vacuo to give a brown-orange oil. This oil was dissolved in H_2O (4 mL), NaCl (5.57 mg, 0.095 mmol) was added and the resulting mixture was stirred at room temperature for 24 h. The solvent was removed under reduced pressure to give a brown solid, which was taken up in MeCN. The suspension was filtered off, and Et_2O was allowed to diffuse into the filtrate to give dark red crystals (8.2 mg, 19% yield). M.p. 214−220 °C with decomposition. $C_9H_{20}BClF_4N_2PdS_2$ (449.05): calcd. C 24.07, H 4.49, N 6.24; found C 23.85, H 4.24, N 6.10. FAB MS (3-noba): *m*/*z* = 363, 325; calcd. for $[^{106}PdCl(\mathbf{L^4})]^+$ $[M^+]$ 362 and $[^{106}Pd(\mathbf{L^4})]^+$: $[M^+]$ 327. UV/Vis (MeCN): λ_{max} (ε_{max}) = 350 (464), 452 nm (51 dm^3 mol^{-1} cm^{-1}). IR (KBr disc): $\tilde{\nu}$ = 3422 s, 3289 m, 3189 m, 3133 m, 3089 m, 2955 w, 1589 m, 1444 m, 1400 m, 1289 m, 1200 w, 1072 s, 917 w, 805 w, 733 w, 533 m, 522m cm^{-1}.

[Cu(L^1)Cl$_2$]: A mixture of **L^1** (46.9 mg, 0.18 mmol) and $CuCl_2{\cdot}2H_2O$ (30.12 mg, 0.18 mmol) was refluxed in MeCN (15 mL) for 1 h under N_2. The solvent of the resulting green solution was allowed to evaporate and after 2 d green crystals of the complex were formed (46.4 mg, 65.5% yield). M.p. 128−130 °C. $C_{12}H_{20}Cl_2CuN_4S$ (386.82): calcd. C 37.26, H 5.21, N 14.48; found C 37.50, H 5.29, N 14.46. FAB MS (3-noba): *m*/*z* = 350, 315; calcd. for $[^{63}Cu(\mathbf{L^1})Cl]^+$ $[M^+]$ 351 and $[^{63}Cu(\mathbf{L^1})]^+$ $[M^+]$ 316. UV/Vis (MeCN): λ_{max} (ε_{max}) = 250 (1670), 335 (4912), 419 (1093), 716 nm (39 dm^3 mol^{-1} cm^{-1}). IR (KBr disc): 2940 w, 2905 w, 2880 w, 2840 w, 2220 m, 1480 m, 1440 s, 1410 s, 1400 s, 1350 s, 1300 s, 1270 m, 1230 w, 1210 w, 1120 w, 1080 s, 1060 m, 1045 m, 1030 m, 1010 w, 1000 w, 985 s, 970 m, 960 w, 940 m, 880 w, 730 m, 710 w, 525 w, 475 w, 380 w, 365w cm^{-1}.

[Cu(L^3)Cl$_2$]: A solution of $CuCl_2{\cdot}2H_2O$ (48.4 mg, 0.28 mmol) in MeCN (4 mL) was added to a solution of **L^3** (61.5 mg, 0.28 mmol) in MeCN (4 mL). A green solid was immediately formed and the mixture was stirred at room temperature for 2 h. The solid was filtered off, washed with Et_2O and dried under reduced pressure (67.4 mg, 68% yield). Single crystals suitable for X-ray diffraction studies were grown by diffusion of Et_2O vapour into a DMF solution of the green solid. M.p. 158−160 °C with decomposition. $C_9H_{16}Cl_2CuN_2S_2$ (350.80): calcd. C 30.81, H 4.60, N 7.98; found C 30.84, H 4.73, N 8.26. FAB MS (3-noba): *m*/*z* = 314, 279; calcd. for $[^{63}Cu(\mathbf{L^3})Cl]^+$ $[M^+]$ 315 and $[^{63}Cu(\mathbf{L^3})]^+$ $[M^+]$ 280. UV/Vis (MeCN): λ_{max} (ε_{max}) = 251 (530), 281 (327), 347 (1090), 428 (348), 762 nm (34 dm^3 mol^{-1} cm^{-1}). IR (KBr disc): $\tilde{\nu}$ = 2978 w, 2929 m, 2243 s, 1472 s, 1444 s, 1409 m, 1366 m, 1344 m, 1305 m, 1119 m, 1097 m, 1037 m, 961 m, 906 m, 834 w, 819 w, 756 w, 734 w, 671 w, 634 w, 595 w, 527 w, 445w cm^{-1}.

[Cu(L^2)][NO$_3$]$_2$: A solution of $Cu(NO_3)_2{\cdot}3H_2O$ (49.5 mg, 0.21 mmol) in MeCN (2 mL) was added to a solution of **L^2** (53.3 mg, 0.21 mmol) in MeCN/EtOH (1:1, v/v; 10 mL). A blue colour immediately developed and the mixture was stirred at room temperature for 1 h. The solvent was removed in vacuo and the residue repeatedly crystallised from EtOH/Et_2O to give blue block-like crystals (48.3 mg, 55% yield). M.p. 190−192 °C. $C_{12}H_{28}CuN_6O_6S$ (448.00): calcd. C 32.17, H 6.30, N 18.76; found C 31.95, H 6.10, N 18.45. FAB MS (3-noba): *m*/*z* = 385, 323; calcd. for $[^{63}Cu(\mathbf{L^2})(NO_3)]^+$ $[M^+]$ 386 and $[^{63}Cu(\mathbf{L^2})]^+$ $[M^+]$ 324. UV/Vis (MeOH): λ_{max} (ε_{max}) = 281 (3013), 556 nm (102 dm^3 mol^{-1} cm^{-1}). IR (KBr disc): $\tilde{\nu}$ = 3378 s, 3200 s, 3100 s, 2922 m, 2855 m, 1611 w, 1372 s, 1205 w, 1161 w, 1083 m, 1069 m, 1041 m, 1020 m, 923 w, 864 w, 826 w, 729 w, 688 w, 542w cm^{-1}.

[Cu(L^4)Cl]PF$_6$: A solution of $CuCl_2{\cdot}2H_2O$ (23.18 mg, 0.14 mmol) in MeOH (4 mL) was added to a solution of **L^4** (30 mg, 0.14 mmol) in MeOH (4 mL); an intense blue colour developed immediately and the mixture was stirred at room temperature for 2 h. The solvent was partially removed under reduced pressure and a large excess of NH_4PF_6 in MeOH solution was added. The solvent was completely removed and the residue washed with water to give a blue solid that was dried under reduced pressure (22.3 mg, 35% yield). Single crystals suitable for X-ray diffraction studies were obtained by recrystallisation from MeCN/Et_2O. M.p. 168 °C. $C_9H_{20}ClCuF_6N_2PS_2$ (464.35): calcd. C 23.28, H 4.34, N 6.03; found C 23.15, H 4.25, N 5.88. FAB MS (3-noba): *m*/*z* = 318, 283; calcd. for $[^{63}Cu(\mathbf{L^4})Cl]^+$ $[M^+]$ 319 and $[^{63}Cu(\mathbf{L^4})]^+$ $[M^+]$ 284. UV/Vis (MeCN): λ_{max} (ε_{max}) = 240 (1671), 312 (3996), 624 nm (126 dm^3 mol^{-1} cm^{-1}). IR (KBr disc): $\tilde{\nu}$ = 3291 s, 3214 s, 3140 w, 2959 w,

Table 6. Summary of crystal data and refinement results

	[Pd(**L^1**)Cl$_2$]	[Pd(**L^2**)][BF$_4$]$_2$	[Pd(**L^3**)Cl$_2$]	[Pd(**L^4**)Cl]BF$_4$	[Cu(**L^1**)Cl$_2$]	[Cu(**L^2**)][NO$_3$]$_2$	[Cu(**L^3**)Cl$_2$]	[Cu(**L^4**)Cl]PF$_6$
Empirical formula	$C_{12}H_{20}Cl_2N_4PdS$	$C_{12}H_{28}B_2F_8N_4PdS$	$C_9H_{16}Cl_2N_2PdS_2$	$C_9H_{20}BClF_4N_2PdS_2$	$C_{12}H_{20}Cl_2CuN_4S$	$C_{12}H_{28}CuN_6O_6S$	$C_9H_{16}Cl_2CuN_2S_2$	$C_9H_{20}ClCuF_6N_2PS_2$
M	429.68	540.46	393.66	449.05	386.82	448.00	350.80	464.35
Crystal size [mm]	0.26×0.21×0.12	0.58×0.37×0.23	0.43×0.39×0.19	0.67×0.31×0.10	0.29×0.12×0.11	0.27×0.27×0.27	0.29×0.19×0.13	0.47×0.24×0.16
Crystal system	monoclinic	orthorhombic	monoclinic	monoclinic	monoclinic	monoclinic	orthorhombic	triclinic
Space group	$P2_1/c$ (no. 14)	$P2_12_12_1$ (no. 19)	$C2/c$ (no. 15)	$P2_1/c$ (no. 14)	$P2_1/n$ (no. 14)	$P2_1/c$ (no. 14)	$Pna2_1$ (no. 33)	$P\bar{1}$ (no. 2)
a [Å]	7.796(3)	9.3480(11)	12.766(2)	12.473(3)	10.758(10)	9.5927(9)	13.9378(7)	7.2762(6)
b [Å]	15.313(4)	13.8508(16)	7.9708(10)	7.389(2)	6.850(9)	13.602(2)	11.9995(8)	9.8513(9)
c [Å]	13.522(2)	15.3511(17)	26.698(3)	17.786(3)	21.56(4)	14.6767(13)	8.2728(6)	12.3494(11)
α [°]	90	90	90	90	90	90	90	72.515(6)
β [°]	90.16	90	92.183(15)	107.18(2)	101.38(12)	106.177(8)	90	79.886(5)
γ [°]	90	90	90	90	90	90	90	89.105(6)
V [Å^3]	1614.3(8)	1987.6(4)	2714.8(6)	1566.1(6)	1558(4)	1839.2(3)	1383.6(2)	830.53(13)
Z	4	4	8	4	4	4	4	2
$D_{calcd.}$ [g·cm^{-3}]	1.768	1.806	1.926	1.905	1.650	1.618	1.684	1.857
T [K]	150(2)	220(2)	220(2)	150(2)	150(2)	220(2)	220(2)	220(2)
μ (Mo-K_α) [mm^{-1}]	1.605	1.117	2.043	1.652	1.874	3.132	2.241	7.149
Reflect. collected	2844	3446	4135	2765	2714	4042	3328	2376
Unique. reflect. R_{int}	2844,--	2349, 0.011	2387, 0.021	2765, --	2528, 0.064	2703, 0.031	2023, 0.017	2376, --
*R*1	0.0349	0.0215	0.0253	0.0218	0.0553	0.0542	0.0349	0.0377
*wR*2	0.0765	0.0541	0.0596	0.0528	0.211	0.159	0.0943	0.0982

2921 w, 1586 s, 1474 s, 1409 m, 1206 w, 1152 m, 1080 m, 995 m, 846vs, 730 w, 642 w, 559s cm^{-1}.

Crystallography: A summary of the crystal data and refinement details for the compounds is given in Table 6. The crystals were cooled using an Oxford Cryosystems open-flow dinitrogen cryostat.[41] For all the compounds diffraction data were collected with a Stoë Stadi-4 four-circle diffractometer using ω-θ scans. Data were corrected for Lorentz and polarisation effects and absorption corrections were applied using numerical or ψ-scan methods. For [Pd(**L^1**)Cl$_2$], and [Pd(**L^4**)Cl]BF$_4$ and [Cu(**L^2**)][NO$_3$]$_2$ a Patterson synthesis using *SHELXS-97*[42] provided a satisfactory set of starting parameters for the heavier atoms. The other structures were solved by direct methods using either *SIR92*[43] or *SHELXS*[42] and developed through subsequent difference Fourier synthesis.[44] All non-H atoms were refined anisotropically and H atoms were located from difference Fourier synthesis (solvent methyl H atoms) or introduced at calculated positions and thereafter incorporated into a riding model with $U_{iso}(H) = xU_{eq}(C)$ (x = 1.2 for CH_2, 1.5 for CH_3). For [Cu(**L^2**)][NO$_3$]$_2$ the NO_3^- anions were restrained to planarity and to have equal N−O bond lengths. In the case of [Cu(**L^4**)Cl]PF$_6$ the PF_6^- ion was found to be disordered during refinement. The disorder was modelled by a partial occupancy model over two sites for each of the four F atoms in the equatorial plane with occupancy factors of 0.59 and 0.41. The two F atoms in the axial positions could be treated as ordered. All the P−F bond lengths were restrained to have the same value during refinement. CCDC-181045 to -181052 contain the supplementary crystallographic data for this paper. These data can be obtained free of charge at www.ccdc.cam.ac.uk/conts/retrieving.html [or from the Cambridge Crystallographic Data Centre, 12 Union Road, Cambridge CB2 1EZ, UK; Fax: (internat.) + 44-1223/336-033; E-mail: deposit@ccdc.cam.ac.uk].

Acknowledgments

We thank the EPSRC and the University of Nottingham for financial support and the EPSRC Mass Spectrometry Service at the University of Swansea for mass spectra.

[1] P. Chaudhuri, K. Wieghardt, *Prog. Inorg. Chem.* **1987**, *35*, 329−436.
[2] P. V. Bernhardt, G. A. Lawrance, *Coord. Chem. Rev.* **1990**, *104*, 297−343.
[3] A. J. Blake, M. Schröder, *Adv. Inorg. Chem.* **1990**, *35*, 1−80.
[4] J. P. Danks, N. R. Champness, M. Schröder, *Coord. Chem. Rev.* **1998**, *174*, 417−468.
[5] K. P. Wainwright, *Coord. Chem. Rev.* **1997**, *166*, 35−90.
[6] A. J. Blake, I. A. Fallis, R. O. Gould, S. Parsons, S. A. Ross, M. Schröder, *J. Chem. Soc., Chem. Commun.* **1994**, 2467−2469.
[7] A. J. Blake, J. P. Danks, V. Lippolis, S. Parsons, M. Schröder, *New J. Chem.* **1998**, *22*, 1301−1303.
[8] A. J. Blake, J. P. Danks, A. Harrison, S. Parsons, P. Schooler, G. Whittaker, M. Schröder, *J. Chem. Soc., Dalton Trans.* **1998**, 2335−2340.
[9] A. D. Pidwell, S. R. Collinson, S. J. Coles, M. B. Hursthouse, M. Schröder, D. W. Bruce, *Chem. Commun.* **2000**, 955−956.
[10] L. Tei, G. Baum, A. J. Blake, D. Fenske, M. Schröder, *J. Chem. Soc., Dalton Trans.* **2000**, 2793−2799.
[11] A. J. Blake, D. W. Bruce, J. P. Danks, I. A. Fallis, D. Guillon, S. A. Ross, H. Richtzenhain, M. Schröder, *J. Mat. Chem.* **2001**, *11*, 1011−1018 and references therein.
[12] W. S. Striejewske, R. R. Conry, *Chem. Commun.* **1998**, 555−556.
[13] D. Parker, A. S. Craig, G. Ferguson, A. J. Lough, *Polyhedron* **1989**, *8*, 2951−2952.
[14] D. G. Fortier, A. McAuley, *Inorg. Chem.* **1989**, *28*, 655−662.
[15] L. R. Gaham, G. A. Lawrance, A. M. Sargeson, *Aust. J. Chem.* **1982**, *35*, 1119−1131.
[16] G. Hunter, A. McAuley, T. W. Whitcombe, *Inorg. Chem.* **1988**, *27*, 2634−2639.
[17] A. J. Blake, L. M. Gordon, A. J. Holder, T. I. Hyde, G. Reid, M. Schröder, *J. Chem. Soc., Chem. Commun.* **1988**, 1452−1454.
[18] A. J. Blake, A. J. Holder, Y. V. Roberts, M. Schröder, *J. Chem. Soc., Chem. Commun.* **1993**, 260−262.
[19] U. Heinzel, R. Mattes, *Inorg. Chim. Acta* **1992**, *194*, 157−161.
[20] U. Heinzel, R. Mattes, *Polyhedron* **1991**, *10*, 19−25.
[21] A. J. Blake, R. D. Crofts, B. DeGroot, M. Schröder, *J. Chem. Soc., Dalton Trans.* **1993**, 485−486.
[22] C. R. Lucas, W. Liang, D. O. Miller, J. N. Bridson, *Inorg. Chem.* **1997**, *36*, 4508−4513.
[23] A. R. Rossi, R. Hoffmann, *Inorg. Chem.* **1975**, *14*, 365−374.
[24] A. J. Blake, A. J. Holder, T. I. Hyde, Y. V. Roberts, A. J. Lavery, M. Schröder, *J. Organomet. Chem.* **1987**, *323*, 261−270.
[25] A. J. Blake, Y. V. Roberts, M. Schröder, *J. Chem. Soc., Dalton Trans.* **1996**, 1885−1895.
[26] B. Chak, A. McAuley, T. W. Whitcombe, *Can. J. Chem.* **1994**, *72*, 1525−1532.
[27] K. Wieghardt, H.-J. Küppers, E. Raabe, C. Krüger, *Angew. Chem. Int. Ed. Engl.* **1986**, *25*, 1101−1103.
[28] S. Chandrasekhar, A. McAuley, *Inorg. Chem.* **1992**, *31*, 2663−2665.
[29] G. J. Grant, K. A. Sanders, W. N. Setzer, D. G. VanDerveer, *Inorg. Chem.* **1991**, *30*, 4053−4056.
[30] A. J. Blake, R. O. Gould, A. J. Lavery, M. Schröder, *Angew. Chem. Int. Ed. Engl.* **1986**, *25*, 274−276.
[31] G. Reid, A. J. Blake, T. I. Hyde, M. Schröder, *J. Chem. Soc., Chem. Commun.* **1988**, 1397−1399.
[32] H. Nikol, H.-B. Bürgi, K. I. Hardcastle, H. B. Gray, *Inorg. Chem.* **1995**, *34*, 6319−6322.
[33] R. D. Hancock, S. M. Dobson, J. C. A. Boeyens, *Inorg. Chim. Acta* **1987**, *133*, 221−231.
[34] J. C. A. Boeyens, S. M. Dobson, R. D. Hancock, *Inorg. Chem.* **1985**, *24*, 3073−3076.
[35] L. R. Gahan, C. H. L. Kennard, G. Smith, T. C. W. Mak, *Transition Met. Chem.* **1986**, *11*, 465−466.
[36] A. J. Blake, J. P. Danks, I. A. Fallis, A. Harrison, W.-S. Li, S. Parsons, S. A. Ross, G. Whittaker, M. Schröder, *J. Chem. Soc., Dalton Trans.* **1998**, 3969−3976.
[37] A. J. Blake, J. P. Danks, W.-S. Li, V. Lippolis, M. Schröder, *J. Chem. Soc., Dalton Trans.* **2000**, 3034−3040.
[38] K. Wasielewski, R. Mattes, *Acta Crystallogr., Sect. C* **1990**, *46*, 1826−1828.
[39] L. Tei, A. J. Blake, P. A. Cooke, C. Caltagirone, F. Demartin, V. Lippolis, F. Morale, C. Wilson, M. Schröder, *J. Chem. Soc., Dalton Trans.* **2002**, 1662−1670.
[40] V. Lippolis, A. J. Blake, P. A. Cooke, F. Isaia, W.-S. Li, M. Schröder, *Chem. Eur. J.* **1999**, *5*, 1987−1991.
[41] J. Cosier, A. M. Glazer, *J. Appl. Crystallogr.* **1986**, *19*, 105−107.
[42] *SHELXS*-86 and *SHELXS*-97: G. M. Sheldrick, *Acta Crystallogr., Sect. A* **1990**, *46*, 467−473.
[43] A. Altomare, M. C. Burla, M. Camelli, G. Giacovazzo, A. Guagliardi, G. Polidori, *J. Appl. Crystallogr.* **1994**, *27*, 435−436.
[44] G. M. Sheldrick, *SHELXL*-93 and *SHELXL*-97, *Programs for Crystal Structure Refinement*, University of Göttingen, Germany, **1993** and **1997**.

Received September 10, 2002
[I02506]